Songklanakarin J. Sci. Technol.
34 (1), 61-67, Jan. - Feb. 2012

SONGKLANAKARIN JOURNAL OF SCIENCE AND TECHNOLOGY
http://www.sjst.psu.ac.th

Original Article

A study of diffuser angle effect on ducted water current turbine performance using CFD

Palapum Khunthongjan* and Adun Janyalertadun

Department of Mechanical Engineering, Faculty of Engineering, Ubon Ratchathani University, Mueang, Ubon Ratchathani, 34190 Thailand.

Received 9 March 2011; Accepted 26 October 2011

Abstract

The water current has used as the energy resource for long time however its velocity is very low therefore there are not found in wide range of uses. This study purposes accelerate water velocity by installing diffuser. The problems were analyzed by one dimension analysis and computational fluid dynamics (CFD); the domain covers the diffuser and turbine which substituted by porous jump condition is install inside. The flow was identified as axisymmetric steady flow, the inlet boundary is identified as uniform flow, all simulation use the same size of diffuser, only the diffuser angles are vary. The results show that velocities of water current in diffuser are increase when the diffuser angle are widen. The angle of diffuser is 20°, the velocity is increase to 1.96 times, compared to free stream velocity. If the angle was about 0-20° and 50-70° the force toward diffuser became high instantly; where as the force toward the rotor will be still and the maximum rate of diffuser augmentation possibly was 3.62 and rotor power coefficient was 2.14.

Keywords: water current turbine, diffuser, computational fluid dynamics, power augmentation, ducted water turbine

1. Introduction

The uses of kinetic energy of water current for generating electricity or pumping has been studied for a long times, which mainly aims to use in remote areas (Fraenkel, 2006; Ponta and Jacovki, 2008; Ponta and Dutt, 2000; Myyers and Bahaj, 2006; Bahaj and Myers 2003; Khan *et al.*, 2008; Kiho *et al.*,1999; G MacPherson-Grant, 2005). According to the kinetic energy use from water current, commercial wind turbine-based knowledge can appropriately be applied where its capacity of energy distribution is as Betz limit. The wind turbine has its maximum power coefficient, $C_P = 0.59$, defined as energy produced by wind turbine per total energy available of wind. Although its capacity was 45% developed, it still challenges the researcher to continue strengthen the effectiveness.

A setup of diffuser is a choice to increase the efficiency that can be with both wind and water turbines as found in the wind turbine study by Phillips *et al.* (2002) from the University of Auckland, New Zealand, Toshiio Matsushima *et al.* (2006) and Yuji Ohya *et al.* (2008). The study of Gerald and Van Bassel (2007) however indicates no any power augmentation factor was more than 3, while as in the theory the power coefficient probably was 2.5; but the price of a diffuser is somewhat high.

David *et al.* (2008) were applying diffusers to water turbine that points to a 1.3 times increase of the output power of the bare turbine by installing a duct. Kirke (2005) shows in the examination of the axial flow turbine that a slotted duct installed in a towing tank tells to increase 70% of the output power if compared to a bare turbine. Grant (2005) reported that the ducted turbine was capable to pay a double load of the duct uninstalled turbine.

In addition, several countries, Canada, Ireland, England, U.S.A., Australia, and Portugal, have been developing water turbines for electricity, which are all in process, for

* Corresponding author.
Email address: pakhunthongjan@gmail.com

examining the model mechanics, and for commercial use.

Although the capacity of water current at low flow velocity, to be used as the energy source, is seldom applied to a water turbine, this article means to study functions and performance of a diffuser as to be the output power accelerator of horizontal axis water current turbine at low flow velocity, in order to be applied in the Northeast of Thailand that has two main rivers, the Moon and the Chii. The velocity of the water current is between 0-1.3 m/s, which is transformed into a two dimensional system by computational fluid dynamic (CFD). The attractive factors are the effect of diffuser angle, maximum augmentation factor, and rotor power coefficient due to the use of the diffuser design for a water current turbine.

2. Materials and Methods

2.1 One dimensional analysis

The one dimensional analysis is based on van Bassel (2007)

1) Empty diffuser case

From Figure 1 the surface of the diffuser outlet will be the reference point, front and back space of diffuser equals atmospheric pressure (P_0). The Bernoulli equation shows that the total pressure equals

$$P_{tot} = P_0 + \frac{1}{2}\rho V_0^2 = P_1 + \frac{1}{2}\rho V_1^2 = P_3 + \frac{1}{2}\rho V_3^3 = P_0 + \frac{1}{2}\rho V_e^2 \tag{1}$$

From the continuity equation the coherence between the inlet velocity (V_1), outlet velocity (V_3), and diffuser area ratio (β) is

$$V_1 = \beta V_3 \tag{2}$$

$$V_3 = \gamma V_0 \tag{3}$$

2) In terms of installed the rotor turbine:

$$V_3 = \gamma(1-a)V_0 \tag{4}$$

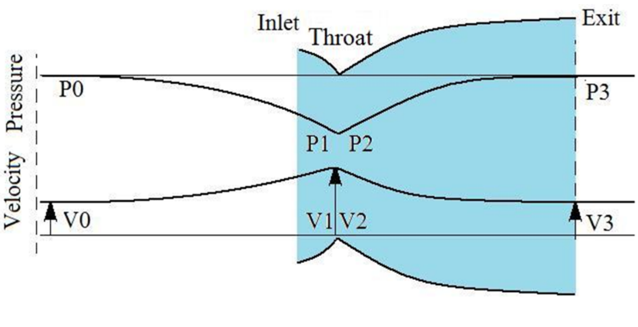

Figure 1. Relationship between pressure and velocity within the empty diffuser

$$V_1 = \beta\gamma(1-a)V_0 \tag{5}$$

The axial induction factor a is defined as $a = (V_0 - V_3)/V_0$, rotor power coefficient $C_{P,R}$ is defined as $C_{P,R} = \beta\gamma 4a(1-a)^2$, power coefficient at diffuser exit $C_{P,exit}$ is defined as $C_{P,exit} = \gamma 4a(1-a)^2$, total thrust coefficient $C_{T,T}$ is defined as $C_{T,T} = \beta\gamma 4a(1-a)$, and thrust coefficient of diffuser $C_{T,D}$ is defined as $C_{T,D} = C_{T,T} - C_{T,R} = (\beta\gamma - 1)4a(1-a)$.

2.2 Computational fluid dynamics

Computational Fluid Dynamics (CFD) is a branch of fluid mechanics that uses numerical methods and algorithms to solve and analyze problems that involve fluid flows. Computers are used to perform the calculations required to simulate the interaction of liquids or gases with surfaces defined by boundary conditions. There are three main processes – pre-processing, calculation processing, and post-processing. Here the Fluent 6.3 commercial code 2 dimensions with the finite volume method was used.

Governing equations

In this study, the Reynolds-Average-Naviaers–Stokes (RANS) equation is considered with renormalization group $k-\varepsilon$ turbulence model, which are indicated in Equation 6 to 11.

Continuity:

$$\frac{\partial}{\partial x_i}\left(\rho \overline{u_i}\right) = 0 \tag{6}$$

Momentum:

$$\frac{\partial}{\partial x_j}\left(\overline{\rho u_i u_j}\right) = -\frac{\partial \overline{p}}{\partial x_i} + \frac{\partial}{\partial x_j}\left[\mu_\tau\left(\frac{\partial \overline{u_i}}{\partial x_j} + \frac{\partial \overline{u_j}}{\partial x_j} - \frac{2}{3}\delta_{ij}\frac{\partial \overline{u_l}}{\partial x_l}\right)\right] + \frac{\partial}{\partial x_j}\left(-\rho\overline{u_i' u_j'}\right) \tag{7}$$

In Equations 6 and 7 $\overline{p}$ is the mean pressure, $\overline{u}$ is the mean velocity, μ is the molecular viscosity, and $-\rho\overline{u_i' u_j'}$ denotes the Reynolds stress. To correctly account for turbulence, Reynolds stress is modeled utilizing the Boussineq hypothesis to relate the Reynolds stress to mean velocity gradients within the flow. The Reynolds stress is defined as:

$$-\overline{\rho u_i' u_j'} = \mu_t\left(\frac{\partial \overline{u_i}}{\partial x_j} + \frac{\partial \overline{u_j}}{\partial x_i}\right) - \frac{2}{3}\left(\rho k + \mu_t \frac{\partial \overline{u_i}}{\partial x_i}\right)\partial_{ij} \tag{8}$$

where μ_t is the turbulent viscosity and k is the turbulent kinetic energy. For k-ε in the turbulence model the turbulent viscosity is computed through the solution of two transport equations for turbulent kinetic energy and turbulence dissipation rate ε_t. The RNG transport equations are

$$\frac{\partial g}{\partial t}(\rho k) + \frac{\partial}{\partial x_i}\left(\rho k \overline{u_i}\right) = \frac{\partial}{\partial x_j}\left[\alpha_k \mu_{eff}\frac{\partial k}{\partial x_j}\right] + G_k + G_b - \rho\varepsilon - Y_M + S_k \tag{9}$$

$$\frac{\partial}{\partial t}(\rho\varepsilon) + \frac{\partial}{\partial x_i}\left(\rho\varepsilon \overline{u_i}\right) = \frac{\partial}{\partial x_j}\left[\alpha_k \mu_{eff}\frac{\partial \varepsilon}{\partial x_j}\right] + C_{1\varepsilon}\frac{\varepsilon}{k}\left(G_k + C_{3\varepsilon}G_b\right) - C_{2\varepsilon}\rho\frac{\varepsilon^2}{k} - R_\varepsilon + S_\varepsilon \tag{10}$$

$$R_\varepsilon = \frac{C_\mu \rho \eta^3 (1-\eta/\eta_0)}{1+\beta\eta^3}\frac{\varepsilon^3}{k} \tag{11}$$

Computational conditions

The domain of the flow problem will cover diffuser and turbine area that are specified as wall and porous jump condition. The inlet boundary is set as the uniform flow velocity, the outlet boundary is set as outflow, top wall is as moving (slip) wall instead of volume of fluid (VOF) model, because of less time for calculation and acceptable accuracy, and the bottom wall is set as axisymmetric shown in Figure 2 and 3. Domains will be drawn in the Gambit program before been computerized by Fluent 6.3. Problem domains will be separated by quadrilateral grids into approximately 11,000 cells. Anyhow, grids will be dense around diffuser wall and turbine area.

The study sets the flow as axisymmetric steady flow it is segregated solver, whereas the turbulence model is a RNG k-ε model. The standard near wall function was chosen for the near wall treatment method with 10^{-6} of the convergence criterion. Sizes of the diffuser are unchanged but the diffuser angle shown in Figure 3 was changed from 0-90°. The porous medium will be from Darcy's Law and an additional inertial loss term with the equation as follows:

$$\Delta p = \left(\frac{\mu}{\alpha}v + C_2\frac{1}{2}\rho v^2\right) \tag{12}$$

where μ is the laminar fluid viscosity, α is the permeability of the medium, C_2 is the pressure-jump coefficient, υ is the velocity normal to the porous face, and Δm is the thickness of the medium.

3. Results and Discussion

3.1 Simulation results

Y^+ check:

In order to set the fineness of partition of the grid the refinement factor equals and when Re>100,000, the flow regime is turbulent and for the standard wall functions the proper Y^+ value is >30. From Figure 4 Y^+ of the diffuser wall values are from 26 to 398.

The evaluation of grid and Reynolds numbers per domain is split into 11,000 and 7,100 quadrilateral cells and the calculated Reynolds number is at 1,800,000 and 2,400,000, respectively. The Reynolds number was defined as VD/υ where V is the axial velocity in m/s, D is the diameter of the diffuser and υ is the kinematic viscosity of water. Its result are an increased velocity (V_1/V_0) and a pressure coefficient (C_p) that is slightly different as shown in Figure 5 and 6, which will be cited later.

Flow inside the Diffuser

The results show that the differential pressure between upstream, in front of the diffuser, and downstream, at the end of the diffuser, increase when the diffuser angle is increased as shown in Figure 6a. The velocity of the water at the throat therefore is increasing varying with an increase of

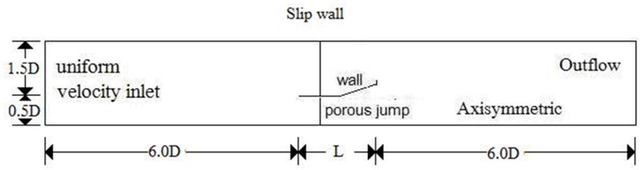

Figure 2. Domain of the problem

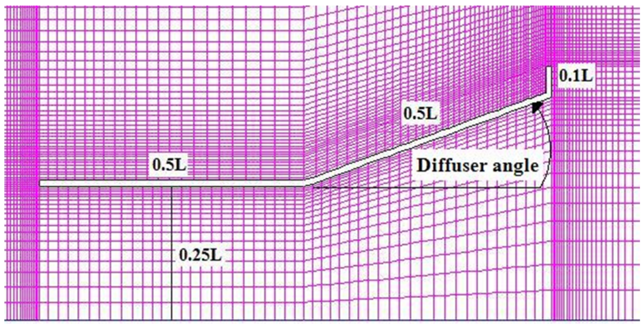

Figure 3. Diffuser dimension and grid system

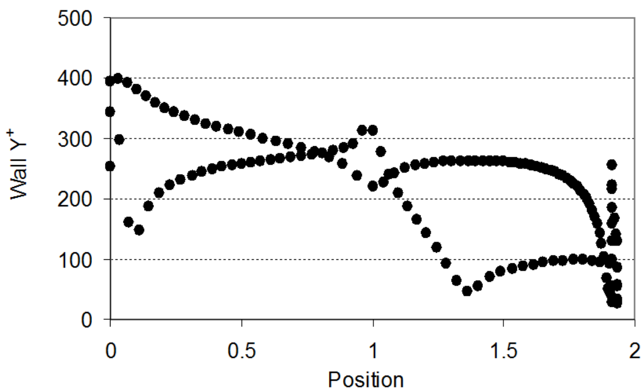

Figure 4. Y^+ of diffuser wall.

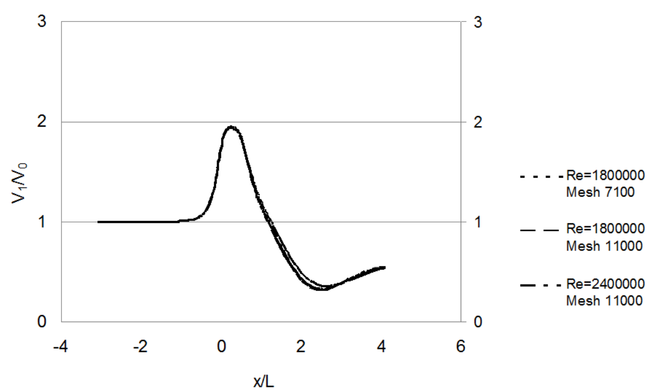

Figure 4.1 V_1/V_0 at axial diffuser.

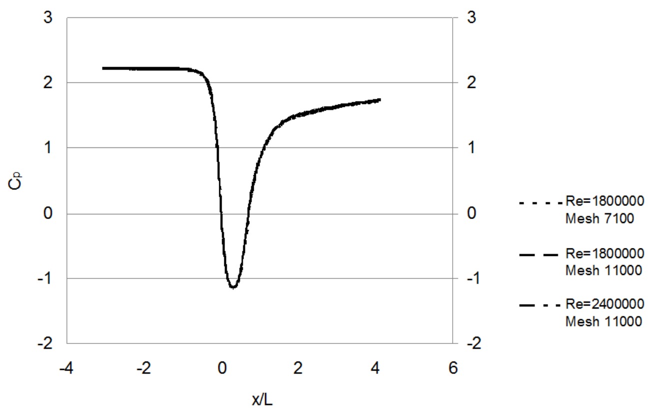

Figure 5. Value of C_p at axial diffuser.

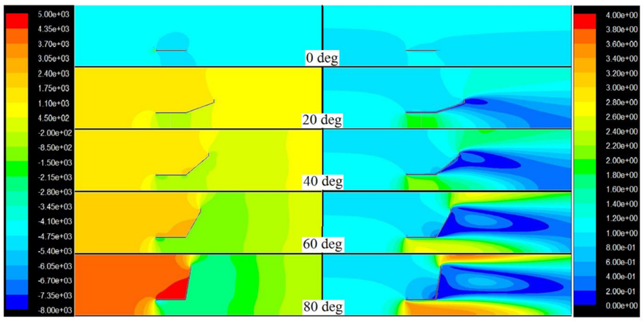

(a) Static pressure (pascal) (b) Velocity (m/s)

Figure 6. Velocity (a) and pressure contour (b) of the empty diffuser.

the diffuser angle as shown in Figure 6b. However, the flow pattern can be divided into two cases: the first group is when the diffuser angles are between 0 and 20 degrees, which are the reasons for the increase in velocity at the throat because the pressure at the back of the diffuser becomes negative pressure due to the diffuser angle as shown in Figure 6a. The fluid flow at the throat will try to maintain its flow condition and accelerated through diffuser and the maximum speed is in the diffuser as shown in Figure 6b. The other group is the case of higher degrees, 40, 60 and 80 degree, even though the axial exit velocity does not decrease but the recirculation occurred at the exit of the diffuser. This recirculation also caused of lower pressure, then fluid in diffuser try to decrease pressure to exit value and fluid is speed up inside. That all results agree with Abe, Ohya, 2004

When rotor turbine was installed in diffuser. Equation (12) was used to find out load of rotor. The 1st term is assumed to be zero. Maximum turbine power coefficient from Betz theory is 0.59 when induction factor (a) is 1/3, then C_2 equals 1333 /m at porous medium of 0.0015 m thickness.

The results of 2D Simulation show the streamline, at the angle of diffuser at 0°, 20°, and 80°, of empty diffuser and diffuser with 0.59 Cp of rotor turbine as shown in Figure 7a) and 7b), respectively. The increasing angle of diffuser shows the increasing of effective area. Even though when the rotor was installed, this area is not much changed. This is the reason the velocity increased in the diffuser and there was more recirculation at exit of duct. However when the rotor turbine is installed, the flow shows the increase of recirculation with increasing diffuser angle.

The relation of velocity inside diffuser also show in the results of velocity plot on x -axis with different diffuser angle as shown in Figure 8. These results confirm all previous results that the velocity inside diffuser increases when the diffuser angle increases.

3) Diffuser augmentation, $\beta\gamma$

The results show diffuser area ratio, (β) Back pressure velocity ratio, (γ), Diffuser augmentation ($\beta\gamma$), VS Diffuser angle. β increases up to approximately 1.75 at 20 degree and then decreases to 1.0 at 50 degree, while γ gets increasing when the angle of diffuser increases as shown in Figure 9. It means that there is negative back pressure at the exit of the diffuser as seen in Figure 10. But the multiplication of β and γ is up. Therefore, it can be defined as γ significantly effects on diffuser augmentation ($\beta\gamma$) while β will be important if its angle is less than 20°

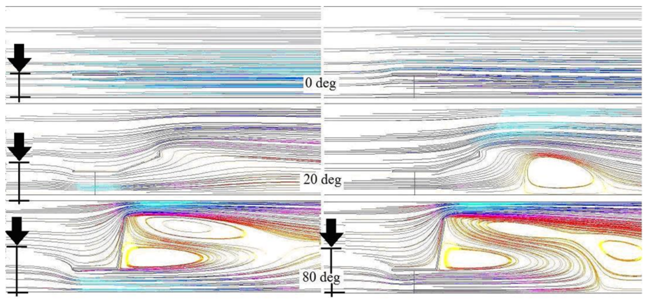

(a) (b)

Figure 7. Water streamlines of diffuser (a) without and (b) with 0.59 Cp of rotor turbine at 0, 20, and 80 degree.

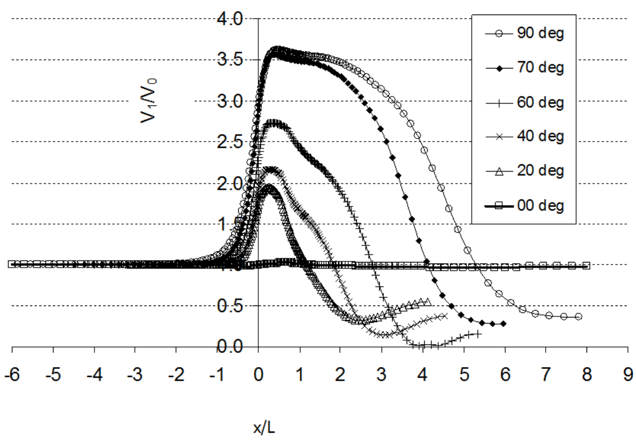

Figure 8. Relation between V_1/V_0 at different points on the x-axis direction to angle of the empty diffuser.

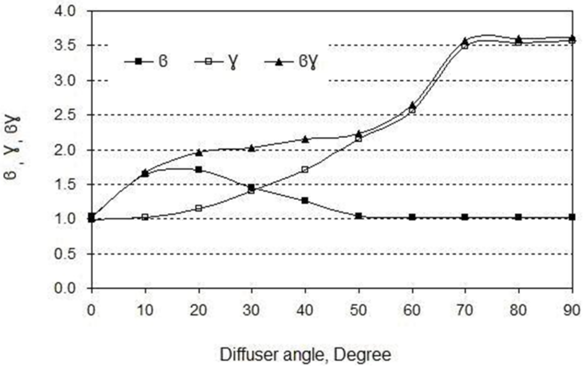

Figure 9. Relation of the diffuser area ratio, (β), back pressure velocity ratio, (γ), and diffuser augmentation, ($\beta\gamma$) to diffuser angle.

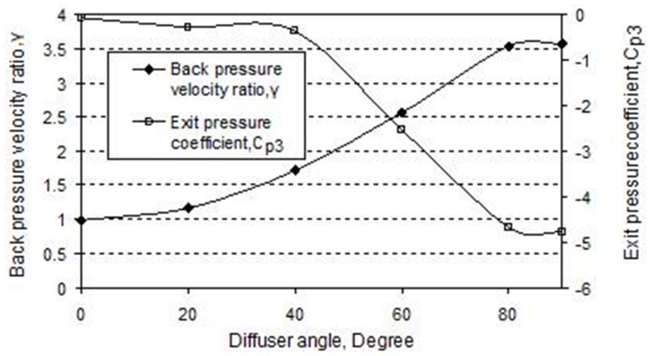

Figure 10. Relation of back pressure velocity ratio, (γ), and exit pressure coefficient, $C_{P,Exit}$, to diffuser angle.

4) Axial flow

The results also show From Figure 11 we can see that water speed up strike to rotor with diffuser compare to uninstall or installation of 0 degree diffuser. When V_1/V_0 increased according to angle of diffuser, pressure drop across rotor of turbine increased too. This show system can produce more power when more angle of diffuser was installed to rotor

5) Thrust loading coefficient

Figure 12: to widen angle of diffuser causes diffuser augmentation be higher; while thrust forced toward diffuser is obviously getting up between the phase of 0-20° and 50-70° but slightly influence on thrust coefficient of rotor. It can be defined as if we build diffuser with the more degree in order to keep energy as much as we require, durable structure is needed for the increasing thrust.

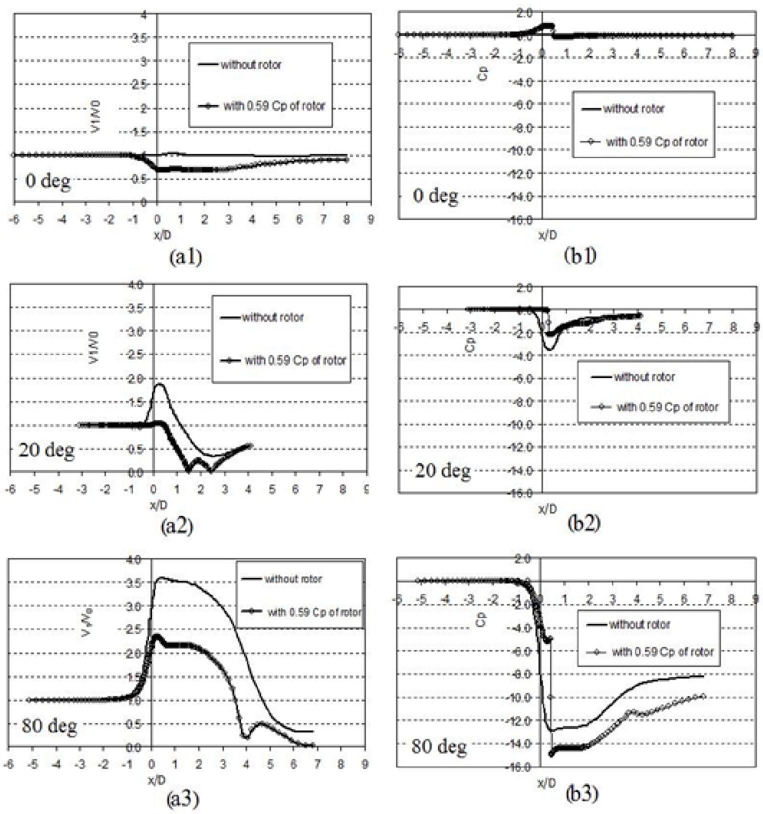

Figure 11. Velocity (a) and pressure coefficient (b) at axis of diffuser with and without rotor turbine with 0, 20, and 80 degree of the diffuser.

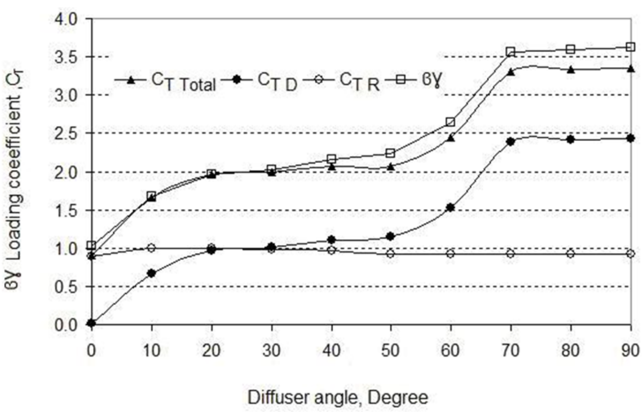

Figure 12. Relation of disk loading coefficient, $C_{T,Total}$, $C_{T,D}$, $C_{T,R}$, and $\beta\gamma$ to diffuser angle, in degree.

6) Rotor power coefficient

Figure 13: It shows the Rotor power coefficient and diffuser augmentation, $\beta\gamma$ in case of axial induction factor, a = 1/3.We will see that the Maximum rotor power coefficient is 2.14 at 90 degree, and the minimum is 0.59 at 0 degree (we supposed it is the ideal turbine). We can say that the diffuser augmented rotor power 3.62 times compared to the system without the diffuser

7) Validation of model

To validate the model simulation, 1.1 meter diameter 20 degree of diffuser was constructed and test in natural flow channel. Velocity of free upstream and middle of diffuser was collected every 20 second by paddlewheel flow sensor IP101 series. It was found that at mean free stream in front of diffuser 0.90 m/s we got 1.55 m/s inside of diffuser. We can say that Diffuser augmentation is 1.72 compare to the simulation result 1.96 or 14% different.

4. Concluding remarks

Widening degree of diffuser causes more augmentation of V_1/V_0 which will be rapidly growing during the phase 0-20° and 50-70°. If the degree approximately equals 20°-50°, the augmentation will not change much; while the angle is about 70°-90° V_1/V_0 will be fixed. Thrust toward rotor will be steady if the augmentation is increased; where as thrust toward diffuser will be higher similarly. So, before contouring it's necessary to evaluate thrust. The effective factors towards V_1/V_0 include Diffuser area ratio, (β) and Back pressure velocity ratio (γ) that the latter one indicates it's increasing according to degree of diffuser which is good to performance of diffuser angle. At the same time β will be lower if the angle degree is more than 20° and will 1 as approximation when the degree is up to 50°. Via the study the diffuser augmentation will reach the maximum rate at 3.62 when the angle degree equals 90° and when the angle degree is about 20°- 50° the maximum rotor power coefficient twill be about 2.14

The above study aims at studying single factor that is diffuser angle. Still, there are many important factors needed further studying such as height of flange, length of diffuser and installing technique and etc.

Acknowledgment

The authors thank the Electricity Generating Authority of Thailand for funding this research.

References

Bahaj, A.S. and Myers, L.E. 2003, Fundamentals applicable to the utilization of marine current turbine for energy production, Renewable Energy 28, 2205-2211.

Kirke, B. 2005. Development in ducted water current turbines available online at www. Cyberiad.net

David, L. F., Gaden and Eric L. Bibeau. 2008. Increasing Power Density of inetic Turbines for Cost-effective Distributed Power Generation. Department of Mechanical and Manufacturing Engineering, University of Manitoba,

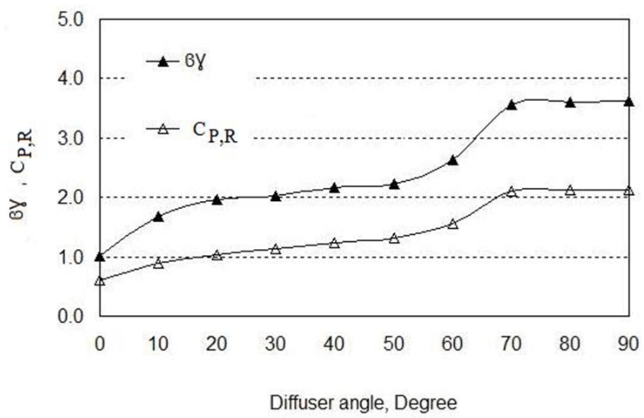

Figure 13. Relation of rotor power coefficient, $C_{P,R}$, and diffuser augmentation, $\beta\gamma$, to diffuser angle, in degree, in case of a = 1/3.

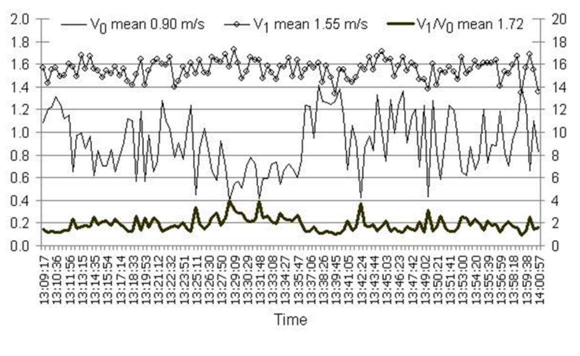

Figure 14. Diffuser without rotor turbine test result.

Canada.

Fernando Ponta and Gautam Shankar Dutt, An improved vertical-axis water-current turbine incorporating a channeling device, Renewable energy 20 (2000), 223-241.

Final Report on Preliminary Works Associated with 1MW Tidal Turbine Project Reference: T/06/00233/00/00 URN 06/2046 Contractors Sea Generation Ltd Prepared by David Ainsworth, Jeremy Thake Marine Current Turbines Ltd.

Gerard, J.W. van bassel. 2007. The science of making more torque from wind: Diffuser experiments and revisited. Journal of physics : conference series 75(2007) 012010 IOP Publishing doi : 10.1088/1742-6596/75/1/012010.

G Mac Pherson-Grant. 2005. (17) The Advantages of Ducted over Unducted Turbines 6th European Wave & Tidal Energy Conference Glasgow, September 2005.

G MacPherson-Grant, The Advantages of Ducted over Unducted Turbines Rotechengineering Ltd.6th European Wave & Tidal Energy Conference Glasgow, September 2005

Ken-ichi Abe, Yuji Ohya. 2004. An investigation of flow field around flange diffuser using CFD, Journal of Wind Engineering and Industrial Aerodynamics 92, 315-330.

Khan M.J., Iqbal M.T. and J.E.Quaicoe. 2008. River current energy conversion system: Progress, prospects and challenges, Reneable and sustainable energy reviews 12, 2177-2193

Kiho, S., Shiono, M. and Suzuki, K. The power generation from tidal currents by Darrieus turbine, Department of Electric Engineering, College of Science & Technology, Nihon University Tokyo, Japan.

Myyers, L., Bahaj, A.S. 2006. Power output performance characteristics of horizontal axis marine current turbine, Renewable energy 31, 197-208.

Fraenkel, P. 2006. Tidal current energy technologies, Marine current turbine limited, the green, stoke giffford, Bristol BS 34 8PD ,UK Ibis 148, 145-151.

Phillips, D.G., Richards, P.J., Flay, R.G.J. 2002. CFD modeling and the Development of the diffuser augmented wind turbine, Wind and Structure, 5(2-4), 267-276.

Ponta, F.L and Jacovki, P.M. 2008. Marine current power generation by diffuser- augmented floating hydro turbines, Renewable energy 33, 665-673.

Phillips, D.G., Richards, P.J., Flay, R.G.J. 2008. Diffuser development for a diffuser augmented wind turbine using computational fluid dynamics. Department of Mechanical Engineering the University of Auckland, New Zealand.

Matsushima, T., Takagi, S., Muroyama, S. 2006. Characteristics of a highly efficient propeller type small wind turbine with a diffuser. Renewable Energy, 31, 1343-1354.

Ohya, Y., Karasudania, T., Sakuraib, A., Abeb, K., Inouec, M. 2008. Development of a shrouded wind turbine with a flanged diffuser. Journalof wind Engineering and Industrial erodynamics, 96, 524-539.

Symbols:

a	Axial induction factor
α_k, α_ε	Inverse effective Prandtl numbers of k and ε consequently
β	Diffuser area ratio
$\beta\gamma$	Diffuser augmentation
C_p	Pressure coefficient
C_{pi}	Pressure coefficient at location
$C_{P,R'}$	Rotor power coefficient
$C_{P,exit}$	Power coefficient at diffuser exit
$C_{T,D}$	Thrust coefficient of diffuser
$C_{T,T}$	Total thrust coefficient of diffuser plus rotor
$C_{T,R}$	Thrust coefficient of rotor
$C_{1\varepsilon}$, $C_{2\varepsilon}$, $C_{3\varepsilon}$	Constant values
ε	Dissipation rate
G_k	Kinematic energy of mean velocity flow
G_b	Kinematic energy of buoyancy flow
γ	Back pressure velocity ratio
k	Turbulence kinetic energy
P_i	Pressure at location i
μ	Molecular viscosity
V_i	Velocity at location i
$\overline{x}$	Mean of x
Y_M	Contribution of the fluctuating dilatation in compressible turbulence to the overall dissipation rate